

Silver-nanoparticle-embedded antimicrobial paints based on vegetable oil

ASHAVANI KUMAR^{1*†}, PRAVEEN KUMAR VEMULA^{2†}, PULICKEL M. AJAYAN^{1*} AND GEORGE JOHN^{2‡}

¹Department of Materials Science and Engineering, Rensselaer Polytechnic Institute, Troy, New York 12180, USA

²Department of Chemistry, The City College of New York, and The Graduate School and University Center of The City University of New York, New York, New York 10031, USA

*Present address: Department of Mechanical Engineering and Material Science, Rice University, Houston, Texas 77005, USA

†These authors contributed equally to this work

‡e-mail: john@sci.ccnycunyu.edu

Published online: 20 January 2008; doi:10.1038/nmat2099

Developing bactericidal coatings using simple green chemical methods could be a promising route to potential environmentally friendly applications. Here, we describe an environmentally friendly chemistry approach to synthesize metal-nanoparticle (MNP)-embedded paint, in a single step, from common household paint. The naturally occurring oxidative drying process in oils, involving free-radical exchange, was used as the fundamental mechanism for reducing metal salts and dispersing MNPs in the oil media, without the use of any external reducing or stabilizing agents. These well-dispersed MNP-in-oil dispersions can be used directly, akin to commercially available paints, on nearly all kinds of surface such as wood, glass, steel and different polymers. The surfaces coated with silver-nanoparticle paint showed excellent antimicrobial properties by killing both Gram-positive human pathogens (*Staphylococcus aureus*) and Gram-negative bacteria (*Escherichia coli*). The process we have developed here is quite general and can be applied in the synthesis of a variety of MNP-in-oil systems.

Common household oil paint, the oldest form of modern paints, uses a binder that is derived from vegetable oils, obtained from linseed or soya bean. Alkyd paints are based on alkyd resins (vegetable-derived drying oils), which contain a variety of polyunsaturated fatty-acid chains, commonly linoleic and linolenic acid and their triglycerides^{1–3}, which undergo free-radical-mediated autoxidation during the curing/drying process^{4,5} (Fig. 1a–c). The use of naturally generated free radicals would enable us to generate paint-based value-added products. Coatings on surfaces of interest decorate or protect the surfaces^{6–8}. In general, several natural oils, drying oils in particular, are excellent coating materials, and when exposed to air, they form a tough scratch-free film as a result of the oxidative drying (lipid autoxidation) process that occurs through a widely accepted ‘free-radical’ mechanism in the presence of atmospheric oxygen^{4,5} (Fig. 1c). In addition, literature reports suggest that free radicals are known to reduce metal salts to their uncharged metal nanoparticles^{9,10} (MNPs). Hence, we took advantage of the free radicals that are generated during the natural drying process of drying oils/alkyd paints for the preparation of silver- and gold-nanoparticle- (AgNP and AuNP) embedded paints (*in situ*); AgNP-embedded paints are of particular interest owing to their potential bactericidal activity.

Several methods have been reported for the preparation of organic–inorganic hybrid materials; most of the techniques used to incorporate metals into polymeric matrices involve either chemical reactions such as reduction¹¹, mixing preformed metal nanoparticles with polymers¹² or complicated physical techniques¹³, such as sputtering¹⁴, plasma deposition¹⁵ and layer-by-layer deposition¹⁶. All of these techniques add time, cost, multi-step synthesis and complexity to the overall process of fabricating metal-particle-doped materials. Hence, the preparation of MNPs

without using external reagents in a single step (*in situ*) by excluding extra purification processes or transfer protocols will have advantages over the present methods. To overcome the above-mentioned hurdles, we have been working on developing efficient supramolecular organic soft materials as hosts for the synthesis and stabilization of inorganic MNPs^{17–19}. Here, we have used the naturally occurring autoxidation/drying process in vegetable-based drying oils as a tool to prepare MNPs *in situ*.

Silver and silver-based compounds are highly antimicrobial by virtue of their antiseptic properties to several kinds of bacterium, including *Escherichia coli* and *Staphylococcus aureus*^{20–22}. Silver-based antimicrobial agents receive much attention, because of the low toxicity of the active Ag ion to human cells^{23,24}, as well as it being a long-lasting biocide with high thermal stability and low volatility. However, although previous studies on silver and AgNPs have revealed some insights into the application of silver in several areas, little is known about the toxicity of AgNPs, where the size and surface area are recognized as important determinants for toxicity. AgNPs have been shown to possess good biocompatibility with mouse fibroblasts and human osteoblasts²⁵, and their use for biological applications has been widely documented²⁶. AgNPs are known to exhibit antibacterial properties and various research groups have investigated the mechanism of AgNP-mediated antibacterial activity^{27,28}. As the size of the silver particles decreases down to the nanoscale regime, their antibacterial efficacy increases because of their larger total surface area per unit volume^{27,28}. One important aspect to consider is that although efficient antibacterial agents have been developed^{29,30}, they often fail to reach commercial needs owing to their complex, multi-step preparation methods and the high cost of production⁶. If the aim is to develop a general, simple (for example, single-step) procedure to make a solid surface

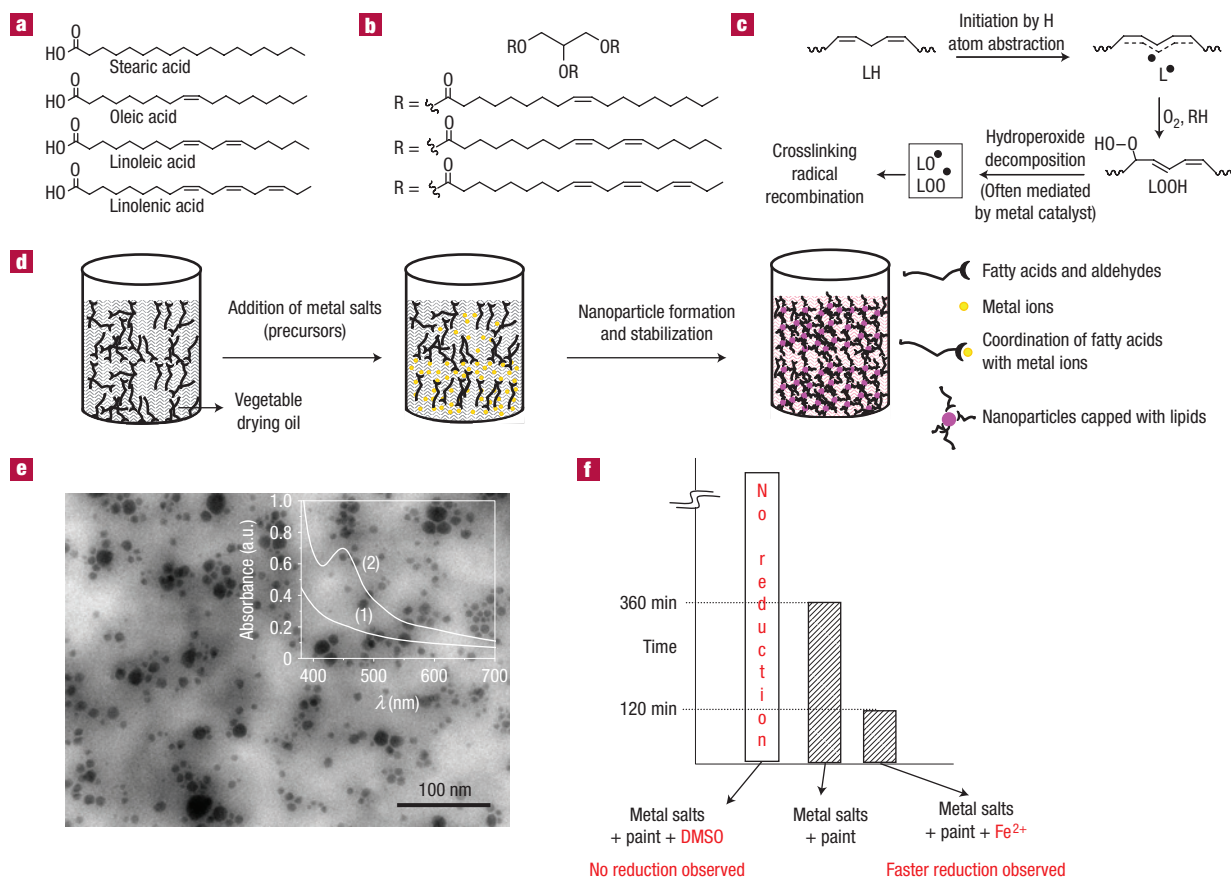


Figure 1 Chemical structure of common fatty acids in drying oils, and synthesis and characterization of AgNPs in alkyd resins. **a**, Chemical structures of fatty acids with different degrees of unsaturation that are present in alkyd resins. **b**, Structures of general triglycerides present in alkyd resins. **c**, General mechanism for the free-radical-mediated autoxidation process in drying oils. **d**, Schematic diagram of *in situ* synthesis and stabilization of MNPs in drying oils. **e**, Transmission electron micrograph of AgNPs synthesized in drying oils with an average size of 12–16 nm. Inset: The absorption spectra of AgNPs with a surface plasmon resonance band; spectra were recorded at (1) 5 min and (2) 24 h after the addition of silver benzoate to the oils. **f**, Kinetics of the metal salt reduction process, time required for nanoparticle synthesis is plotted; the addition of a catalyst (Fe^{2+}) enhanced the generation of free radicals, which increased the rate of nanoparticle synthesis; in contrast, the addition of DMSO, which is a well-known free-radical scavenger, completely prevented nanoparticle synthesis.

bactericidal, then covalent attachment of polymers is probably not a viable option given the paucity of derivatization-amenable functional groups on most common surfaces. Hence, our main aim here is to develop potent antibacterial coatings in a single step at ambient conditions without using external reagents or excessive energy for practical applications. Inspired by the versatility and reliability of oil paints, we decided to explore the use of the oxidative drying mechanism (lipid autoxidation) to generate and stabilize AgNPs in oil paints to compete with previously implemented AgNP-based bactericidal agents^{27,28}.

Typically, nanoparticle synthesis involves external reducing agents and toxic organic solvents, which pose potential environmental and biological risks. However, except for a few reports^{31,32}, it is difficult to find fully environmentally friendly methods for MNP synthesis. Here, by using the naturally occurring autoxidation process³³, we successfully demonstrate an environmentally friendly synthetic protocol for the formation and stabilization of MNPs in paints. The three main steps in the preparation of MNPs that should be evaluated from an environmentally friendly chemistry³⁴ perspective are the choice of the solvent medium used for the synthesis, the selection of an environmentally benign reducing agent and the selection of a non-toxic material for the stabilization of the MNPs. In our

approach, no solvents are required; instead the commercially available environmentally benign drying oils are used. The second concern mentioned above is the choice of the reducing agent. Although there are several reducing agents, the majority of processes reported so far use reducing agents such as sodium borohydride (NaBH_4) and hydrazine ($\text{NH}_2\text{-NH}_2$). All of these are highly reactive chemicals and raise potential environmental and biological risks. In our approach, free radicals that were naturally generated *in situ* during the drying process are used as reducing agents. This process does not require heating, and moreover the system is mild, renewable, cheap and non-toxic in nature. Another and perhaps the most important issue is the choice of a capping agent to protect and passivate the nanoparticle surface, for better dispersion of MNPs. Importantly, in our method, the alkyd resin itself acts as the protecting agent; fatty acids and *in-situ*-generated aldehydes and other intermediates act as stabilizing agents for MNPs.

Free-radical-induced MNP synthesis is well studied^{9,10}. Hence, we predicted that the presence of several *in-situ*-generated free radicals such as LOO^\bullet , LO^\bullet and L^\bullet (L = lipid chain) during autoxidation of drying oils could be useful for the reduction of metal salts to synthesize MNPs *in situ* (Fig. 1c). To test our hypothesis, we used silver benzoate as the precursor for MNPs

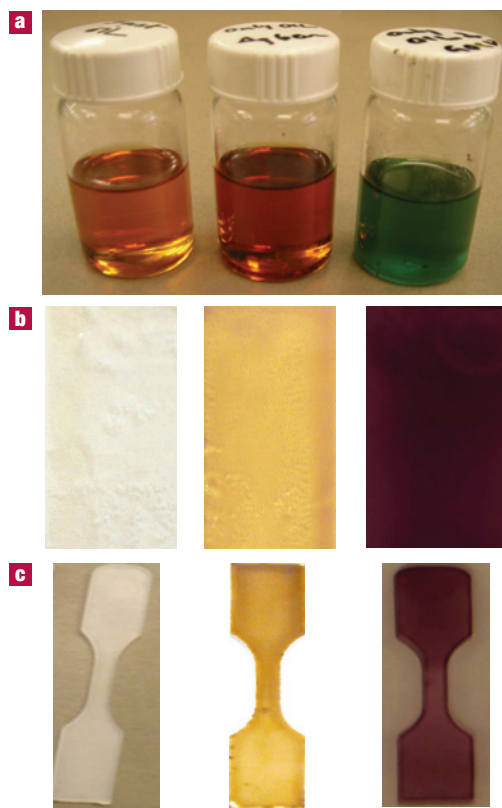


Figure 2 Metal-salt-containing drying oils, and nanoparticle-embedded paint coatings. **a**, Images of plain commercially available drying oil, and silver benzoate and chloroauric acid dissolved in drying oils (left to right). **b,c**, Images of paint coatings without nanoparticles (left panels), with AgNPs (middle panels) and with AuNPs (right panels) on glass (**b**) and polymer (**c**) surfaces.

in drying oil and used the conventional ambient drying process. Interestingly, we observed visual changes: the oil phase became light yellow in colour with time, which indicated the formation of AgNPs. This procedure was also tested for other metal salts; for example, we chose chloroauric acid (HAuCl_4) for AuNP preparation. Appropriate choice of the organometallic salts, for example, silver benzoate, facilitates the solubility of nanoparticle precursors into the oil medium. Hence, it is anticipated that silver salts undergo ligand exchange with fatty acids, which causes the metal ions to dissolve in the oil and subsequent reduction by the free radicals to form nanoparticles^{9,10} (Fig. 1d). To investigate nanoparticle synthesis on surfaces, we coated various surfaces such as glass, polypropylene and poly(methyl methacrylate) with metal-ion-containing drying oils (Fig. 2). After about 6 h of drying at ambient conditions, gold paint turned pink in colour and silver paints turned slightly brownish yellow, indicating the formation of AuNPs and AgNPs in the coatings, respectively. We believe that free radicals generated *in situ* during the autoxidation are responsible for the reduction of metal salts to generate nanoparticles. The presence of AgNPs and AuNPs was confirmed by spectroscopic (ultraviolet–visible) and transmission microscopic techniques. The stability and shelf life of nanoparticles synthesized in drying oils are comparable or even better than those of nanoparticles synthesized using conventional processes (for example, sodium borohydride, citric acid and so on). The higher stability of the nanoparticles is due to the stabilization of the nanoparticles by the polymer matrix formed during the autoxidation. The stability of the nanoparticle

film was confirmed by heating the nanoparticle–oil film at ambient conditions and was quite stable up to 200 °C for an hour without significant aggregation.

To gain further insight into the mechanism of autoxidation of unsaturated alkyl chains that produce free radicals to reduce metal salts, we prepared a synthetic polymer system and explored the metal salt reduction to generate MNPs within the polymer. Cardanol (obtained from thermal treatment of cashew nut shell liquid) is known to exist as a mixture of four components differing in the degree of unsaturation in the side chain: 5% of 3-(pentadecyl)-phenol, 49% of 3-(8Z-pentadecenyl)-phenol, 17% of 3-(8Z,11Z-pentadecadienyl)-phenol and 29% of 3-(8Z,11Z,14Z-pentadecatrienyl)-phenol³⁵ (Fig. 3). A free-radically polymerizable monomer was synthesized from cardanol by simple modifications and was then polymerized. The resulting polymer has an acrylic backbone with many unsaturated alkyl side chains, which are easily amenable to the oxidative drying process, similar to the conventional drying oils^{36,37}. In our previous studies, we demonstrated the oxidative drying (lipid autoxidation) process of poly(cardanyl acrylate) into crosslinked networks by various techniques^{36,37}. To prove the autoxidation-mediated metal salt reduction, we dried poly(cardanyl acrylate) in the presence of HAuCl_4 , which produced a AuNP-embedded crosslinked polymer that was coated on a glass slide (Fig. 3a). As a control experiment, we also synthesized a polymer with a saturated hydrocarbon chain, poly(pentadecylphenyl acrylate) (Fig. 3b). The saturated analogue failed to undergo oxidative drying (lipid autoxidation) owing to the absence of characteristic allylic unsaturation on the polymer side chains, which prevented nanoparticle synthesis. These results clearly support our hypothesis that the autoxidation process of unsaturated chains in drying oils is indeed responsible for the reduction of metal salts.

In-situ-prepared MNP-incorporated alkyd resins were characterized using different techniques including ultraviolet–visible spectrophotometry, transmission electron microscopy, scanning electron microscopy, energy-dispersive X-ray analysis and X-ray photoelectron spectroscopy. The absorption spectrum of nanoparticles generated in oil was monitored as a function of time, as shown in the inset of Fig. 1e. It is clear from the spectra that absorbance at 450 nm increases as a function of time, and this peak appears for the AgNPs owing to the characteristic surface plasmon resonance effect originating from the quantum size of the AgNPs, which again confirms the formation of silver particles at nanoscale dimensions³⁸. The absorbance maximum does not change over a long period, indicating that the silver particles are prevented from coagulating owing to stabilization of nanoparticles by fatty acids, which are essential constituents of the drying oil. Similarly, absorption spectra of *in-situ*-synthesized AuNP-containing oil have shown a surface plasmon resonance peak at 540 nm, characteristic of AuNPs (see Supplementary Information, Fig. S1). Figure 1e shows a representative transmission electron micrograph of AgNPs contained in the films (for more transmission electron micrographs of AgNPs and AuNPs, see Supplementary Information, Fig. S1). The average size of the AgNPs was found to be 12–14 nm; however, larger sizes in the 10–30 nm range were also occasionally observed (Fig. 1e); similarly, the size range for AuNPs is 11–25 nm with a higher polydispersity (see Supplementary Information, Fig. S1). The AgNPs were further characterized using X-ray photoelectron spectroscopy; for a detailed discussion of the X-ray photoelectron spectroscopy results, see Supplementary Information, Fig. S2.

Energy-dispersive X-ray analysis was used to confirm the presence of AgNP- and AuNP-embedded coatings. Thin films of AgNP- and AuNP-incorporated paints on silicon wafers were examined under a scanning electron microscope, and the resulting images are shown in Supplementary Information, Fig. S3, where

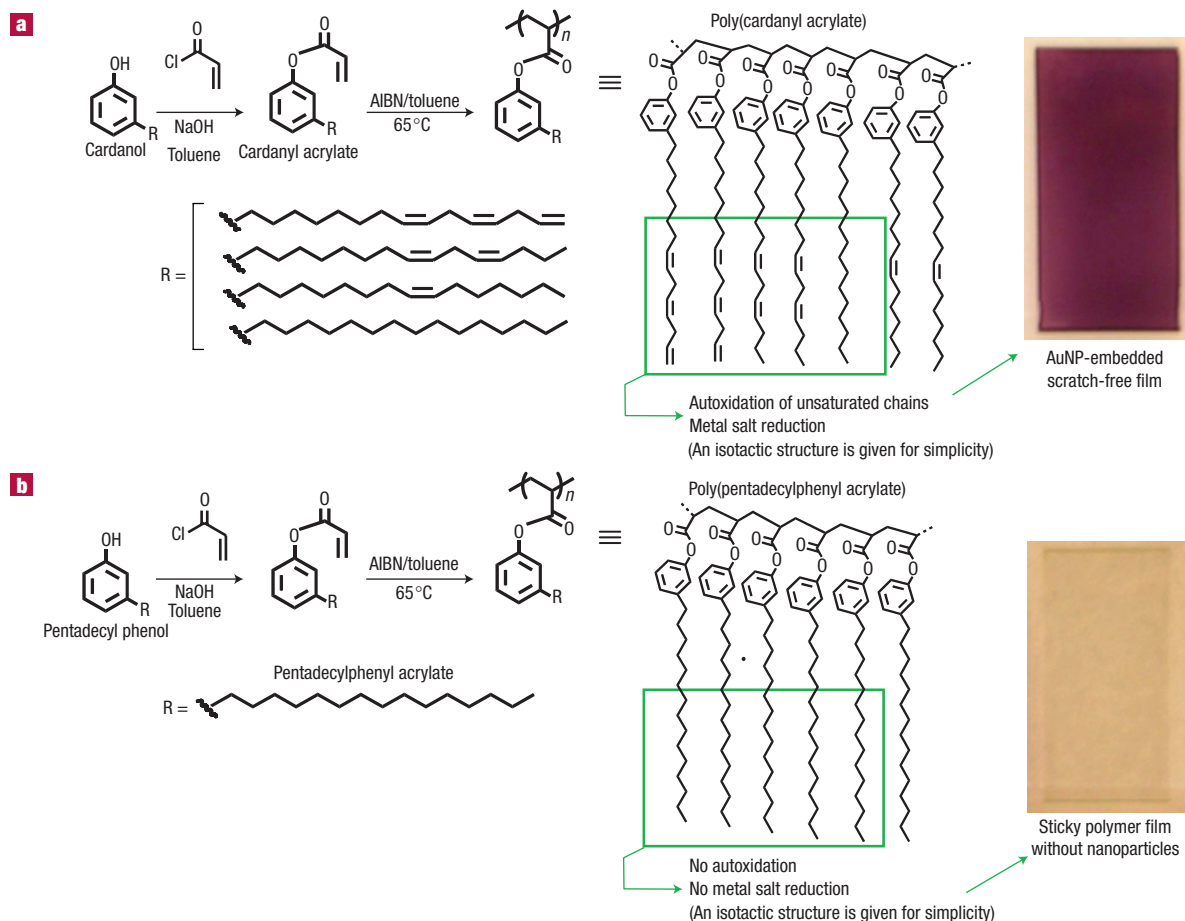


Figure 3 AuNP synthesis in cardanol-based polymer films. **a**, Synthesis of cardanyl acrylate and its polymerization to form poly(cardanyl acrylate) with a mixture of unsaturated alkyl chains, which was used for synthesis of AuNPs (the right image shows the AuNP-embedded polymer film). **b**, Synthesis of pentadecylphenyl acrylate (a saturated analogue), and its polymerization to produce a sticky transparent film that failed to show AuNP synthesis owing to the absence of the autoxidation process (the right image shows the sticky clear polymer film).

it is clear that the surfaces of the coatings were filled with metal nanoparticles (for AgNPs, see Supplementary Information, Fig. S3a and for AuNPs, see Supplementary Information, Fig. S3b). Spot analysis was carried out using energy-dispersive X-ray spectroscopy on the areas where particles were located, in the range of 4 keV, and characteristic peaks at 2.984 keV and 2.195 keV of silver and gold, respectively, were observed. In addition, the background materials showed representative peaks for carbon and oxygen. These results clearly suggest the presence of MNPs embedded in the drying-oil-based paints.

Herein we reason that free radicals generated during autoxidation are responsible for the reduction of metal salts. To shed light on this hypothesis, we carried out two sets of experiments: one to enhance the reduction process by increasing the free-radical generation and the rate of AuNP formation, and the other to completely prevent metal reduction using free-radical scavengers. It is well known that the addition of catalytic metals such as Co(II), Mn(III) and Fe(II) facilitates free-radical formation and subsequently enhances the oxidative drying (lipid autoxidation) process^{39,40}. Hence, we carried out reduction of silver benzoate and chloroauric acid separately by using oil in the presence of Fe(II) ions, where we observed that the kinetics of nanoparticle formation was enhanced threefold

(the Ag^{+1} to Ag^0 reduction time decreased from 360 to 120 min, see Fig. 1f and Supplementary Information, Fig. S4). The kinetics of nanoparticle formation was studied using absorbance spectra measurements of the *in-situ*-synthesized AuNPs (for more spectra and a detailed discussion, see the Supplementary Information). Rate enhancement of nanoparticle formation in the presence of free-radical initiator suggests that free radicals are indeed involved in the reduction process. In the negative control experiments, the reduction process was carried out in the presence of free-radical scavengers. Dimethylsulphoxide (DMSO) is known to act as a free-radical scavenger, and is frequently used to prevent free-radical-mediated processes⁴¹. DMSO (25% v/v) was mixed with the oil, and metal salts were then added and incubated for several months. Intriguingly there was no nanoparticle formation, which was confirmed by absorption spectroscopy. Hence, these results unambiguously suggest that free radicals are indeed mostly responsible for the reduction of metal salts in the drying process. *In-situ*-synthesized MNPs are stable for several months without coagulation, owing to the passivation of MNPs with fatty acids and aldehydes. It is well documented that autoxidation ultimately leads to extensive fragmentation of the fatty-acid chains and generates a variety of biologically active products such as monoaldehydes, γ -ketoaldehydes and 4-hydroxy-nonenal through free-radical

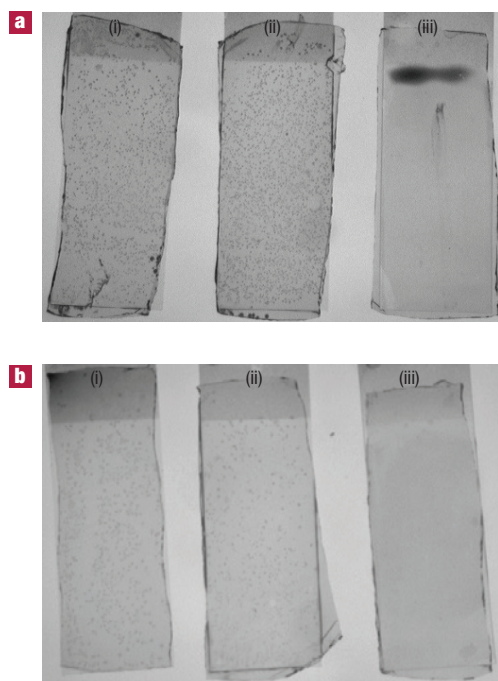


Figure 4 Summary of the antibacterial properties of AgNP-containing paints. **a,b**, Photographs of commercially available blank glass slides without coating (i), glass slides coated with only drying-oil paint without nanoparticles (ii) and glass slides coated with AgNP-containing drying-oil paint (AgNP-embedded paint) (iii), onto which aqueous suspensions of approximately 5×10^6 cells ml^{-1} of *S. aureus* cells (**a**) and 5×10^7 cells ml^{-1} of *E. coli* cells (**b**) in PBS solution were sprayed, followed by drying in air for 5 min, covering with solid growth agar and incubating at 37°C overnight. Each black dot corresponds to a bacterial colony grown from a single surviving bacterial cell.

intermediates^{42,43}; in addition, acids, aldehydes and free radicals are known to interact with MNPs to stabilize them^{18,44,45}. Hence, we believe that the autoxidation reactions produced fragments that bind to *in-situ*-generated MNPs; in addition, the rigid crosslinked polymer (the product of the drying process of oil) also prevents nanoparticle aggregation, resulting in the production of nanoparticle-embedded homogeneous paints.

The AgNP-embedded drying oil is an excellent coating material and can be used to coat several kinds of surface such as wood, glass, polypropylene, poly(methyl methacrylate), polystyrene and building walls made of different materials. As MNPs are homogeneously dispersed in vegetable-based drying oil, the adhesion properties of AgNP- and AuNP-embedded paints were tested by coating them on different substrates such as glass and polymers, as shown in Fig. 2 and Supplementary Information, Fig. S5. To investigate the versatility of this process, we examined several commercially available drying oil/paints such as bleached linseed oil, cold-pressed linseed oil, stand oil and Beckosol oils. In all cases, we could successfully synthesize MNPs *in situ* by using the naturally occurring autoxidation as a tool during the drying process.

Silver is known to exhibit a broad spectrum of biocidal activity towards many bacteria, fungi and viruses^{46,47}. Silver, in its uncharged state (that is, AgNPs) is also found to possess antimicrobial properties. Although the mechanism of this action is still unresolved, it has been shown that AgNPs interact with the constituents of the outer membrane of bacteria, causing structural changes and degradation that eventually lead to the

death of the bacterial cells⁴⁸. AgNPs that are less than 15 nm in size are known to have efficient antibacterial activity^{27,49}. Hence, we reasoned that AgNP-embedded vegetable drying oils may be used as ‘antibacterial paints’ on different surfaces. The bactericidal activity of *in-situ*-synthesized AgNP-embedded vegetable drying oil was explored against both the airborne Gram-positive human pathogen *S. aureus* and its Gram-negative brethren *E. coli*. Here, we prepared surfaces coated with the AgNP-embedded paint by either simple immersion of glass slides (2.5×7.5 cm) into the AgNP-embedded paint or spray coating of AgNP-embedded paint on glass slides followed by drying under air, which produced uniformly coated films. Bacterial colonies were grown on these slides (see the Methods section for details). After overnight incubation of the slides, the bacterial colonies were counted; images of the resulting glass slides are shown in Fig. 4. Each black dot corresponds to an individual bacterial colony. It can be seen in Fig. 4a that the glass slide coated with AgNP-embedded paint killed almost all of the Gram-positive *S. aureus* bacteria compared with both the plain glass slide and the glass slide coated with paint without AgNPs. Similarly, AgNP-embedded vegetable paints were equally active against the Gram-negative *E. coli* bacteria (Fig. 4b). In the case of *E. coli*, control experiments also showed that plain glass and glass coated with paint without AgNPs failed to kill the bacteria, suggesting that AgNPs are indeed responsible for the bactericidal activity. Earlier, Morones *et al.* showed that AgNPs (where silver is present in the Ag^0 form) also contain micromolar concentrations of Ag^+ ions²⁷, and they have shown that Ag^+ and Ag^0 both contribute to the antibacterial activity. To quantify the ratio of Ag^0 to Ag^+ , we carried out X-ray photoemission spectroscopy (for a detailed discussion, see Supplementary Information, Fig. S2). The calculated ratio of Ag^0 to Ag^+ is 7.5:1. Hence, we believe that the silver ions and metallic silver both synergistically contribute to the enhanced antibacterial activity, in agreement with the earlier reports. The proficient bactericidal activity (see Supplementary Information, Table S1) of AgNP-embedded vegetable oil paints against both types of bacterium suggests the use of the present AgNP-incorporated paint formulations in future antibacterial/antimicrobial coatings. All antibacterial tests were carried out in triplicate and were done a minimum of two different times to ensure reproducibility.

METHODS

NANOPARTICLE SYNTHESIS IN OIL

Silver benzoate was purchased from Sigma Aldrich and used as-received. In a typical experiment, 0.034 g of silver benzoate was dissolved in 4.8 g of alkyd paint (all experiments were done with Miniwax, Antique oil finish unless otherwise specified, which was used as-received) and was mixed to form a homogeneous solution and kept at room temperature. Similarly, for the synthesis of AuNPs, 0.136 g of HAuCl_4 was added to 20 ml of drying oil and was mixed with a glass rod to form a green coloured oil, which remained as a gold salt for three weeks. For the MNP synthesis, oil containing metal salts was coated on the glass surfaces and left to dry in air, which caused autoxidation that subsequently led to the formation of MNP-embedded drying-oil scratch-free coatings.

POLY(CARDANYL ACRYLATE) SYNTHESIS

Cardanol was obtained by double vacuum distillation of cashew nut shell liquid at 3–4 mm Hg; the fraction distilled at $230\text{--}235^\circ\text{C}$ was collected. The monomer, cardanyl acrylate and poly(cardanyl acrylate) were synthesized as reported earlier^{36,37}.

NANOPARTICLE SYNTHESIS IN SYNTHETIC POLYMER

Metal salts (silver benzoate or chloroauric acid) were dissolved in acetone, and added to a chloroform solution of poly(cardanyl acrylate). The mixture was coated on the glass slides and left in air to dry, which caused autoxidation and the subsequent formation of MNP-embedded polymeric scratch-free coatings.

TRANSMISSION ELECTRON MICROSCOPY

Transmission electron microscopy data were recorded using a Zeiss EM-902 transmission electron microscope (80 kV). Nanoparticle-embedded oil was placed directly on a 10×10 mm plastic sheet, and after drying at 60°C for 4 h, it was cut using a microtome to obtain 100-nm-thick slices, which were placed directly on a Cu grid and examined under a transmission electron microscope.

SCANNING ELECTRON MICROSCOPY AND ENERGY-DISPERSIVE X-RAY SPECTROSCOPY

A small amount of nanoparticle-embedded oil was placed on a silicon wafer to form a thin layer; the silicon wafer was dried at ambient conditions for 24 h, and was directly examined using a field-emission scanning electron microscope (JEOL-6330F) operated at 5 kV. Energy-dispersive X-ray data were also collected from the same sample at 15 kV using a Prism 2000 Si(Li) X-Ray detector (Princeton Gamma-Tech) coupled with a Zeiss DSM-940 microscope.

ULTRAVIOLET-VISIBLE AND X-RAY PHOTOELECTRON SPECTROSCOPY

Nanoparticle-embedded oil was placed on glass slides and dried to form thin films, which were examined directly with a Perkin Elmer Lambda-950 spectrophotometer operated at a resolution of 2 nm and a PHI-5400 instrument with a 200 W Mg K α probe beam. The spectrometer was configured to operate at high resolution with a pass energy of 20 eV.

BACTERIAL STRAIN AND CULTURE MEDIA

The bacterial strains used were *S. aureus* and *E. coli*. The yeast–dextrose broth contained (per litre of deionized water): 10 g of peptone, 8 g of beef extract, 5 g of NaCl, 5 g of glucose and 3 g of yeast extract. The PBS contained 8.2 g of NaCl and 1.2 g of $\text{NaH}_2\text{PO}_4 \cdot \text{H}_2\text{O}$ per litre of deionized water. The pH of the PBS solution was adjusted to 7.0 with 1 N aqueous NaOH. Both solutions were autoclaved for 20 min before use.

SAMPLE PREPARATION FOR ANTIBACTERIAL STUDIES

Glass slides (2.5×7.5 cm) were coated with the AgNP-embedded paint by either simple immersion into AgNP-embedded paint or spray coating with the AgNP-embedded paint followed by drying in air. Both methods produced uniformly coated glass samples. The slides were left for one day or heated at 60°C for 30 min to make sure that the drying process was complete, so that a scratch-free film was formed. Typically, a 100 μl suspension of *S. aureus* or *E. coli* in 0.1 M PBS (approximately 10^{11} cells ml^{-1}) was added to 20 ml of the yeast–dextrose broth in a 50 ml sterile centrifuge tube, followed by shaking at 200 r.p.m. and 37°C overnight (Innova 4200 Incubator Shaker, New Brunswick Scientific). The bacterial cells were collected by centrifugation at 6,000 r.p.m. for 10 min (Sorvall RC-5B, DuPont Instruments), washed twice with PBS, and diluted to 5×10^6 cells ml^{-1} for *S. aureus* and to 5×10^7 cells ml^{-1} for *E. coli*. To mimic the aerosolized, airborne bacteria, we sprayed the bacterial suspensions in PBS onto slides at a rate of approximately 10 ml min^{-1} in a fume hood. After drying for 2 min in air, the resultant slide was placed in a Petri dish and immediately covered with a layer of solid growth agar (1.5% agar in the yeast–dextrose broth, autoclaved, poured into a Petri dish, and allowed to gel at room temperature overnight). The Petri dish was sealed and incubated at 37°C overnight, and the bacterial colonies grown on the slide surface were counted on a light box. The control experiments investigated the effects of a plain glass surface and paint without AgNPs; both types of bacterial solution were sprayed separately on commercially available glass slides and glass slides coated with oil without AgNPs, respectively.

Received 2 July 2007; accepted 3 December 2007; published 20 January 2008.

References

- Daniel, S. (ed.) *Bailey's Industrial Oil and Fat Products* (Wiley, New York, 1964).
- Metzger, J. O. & Bornscheuer, U. Lipids as renewable resources: current state of chemical and biotechnological conversion and diversification. *Appl. Microbiol. Biotechnol.* **71**, 13–22 (2006).
- Bieleman, J. H. *Additives for Coatings* (Wiley-VCH, Weinheim, 2000).
- Black, J. E. Metal-catalyzed autoxidation. The unrecognized consequences of metal-hydroperoxide complex formation. *J. Am. Chem. Soc.* **100**, 527–535 (1978).
- Reich, L. & Stivala, S. *Autoxidation of Hydrocarbons and Polyolefins* (Marcel Dekker, New York, 1969).
- Bohannon, J. 'Smart coatings' research shows the virtues of superficiality. *Science* **309**, 376–377 (2005).
- Crisp, M. T. & Kotov, N. A. Preparation of nanoparticle coatings on surfaces of complex geometry. *Nano Lett.* **3**, 173–177 (2003).
- Klaus, T., Joergers, R., Olsson, E. & Granqvist, C.-G. Silver-based crystalline nanoparticles, microbially fabricated. *Proc. Natl Acad. Sci. USA* **96**, 13611–13614 (1999).
- Zhang, J. *et al.* Sonochemical formation of single-crystalline gold nanobelts. *Angew. Chem. Int. Edn* **45**, 1116–1119 (2006).
- Okitsu, K. *et al.* Synthesis of palladium nanoparticles with interstitial carbon by sonochemical reduction of tetrachloropalladate(II) in aqueous solution. *J. Phys. Chem. B* **101**, 5470–5472 (1997).

- Aymonier, C. *et al.* Hybrids of silver nanoparticles with amphiphilic hyperbranched macromolecules exhibiting antimicrobial properties. *Chem. Commun.* 3018–3019 (2002).
- Lu, Y., Liu, G. L. & Lee, L. P. High-density silver nanoparticle film with temperature-controllable interparticle spacing for a tunable surface enhanced raman scattering substrate. *Nano Lett.* **5**, 5–9 (2005).
- Heilmann, A. *Polymer Films with Embedded Metal Nanoparticles* (Springer, New York, 2002).
- Dowling, D. P. *et al.* Anti-bacterial silver coatings exhibiting enhanced activity through the addition of platinum. *Surf. Coat. Technol.* **163**, 637–640 (2003).
- Jiang, H., Manolache, S., Wong, A. C. L. & Denes, F. S. Plasma-enhanced deposition of silver nanoparticles onto polymer and metal surfaces for the generation of antimicrobial characteristics. *J. Appl. Polym. Sci.* **93**, 1411–1422 (2004).
- Dai, J. & Bruening, M. L. Catalytic nanoparticles formed by reduction of metal ions in multilayered polyelectrolyte films. *Nano Lett.* **2**, 497–501 (2002).
- Mallia, V. A., Vemula, P. K., John, G., Kumar, A. & Ajayan, P. M. In situ synthesis and assembly of gold nanoparticles embedded glass forming liquid crystals. *Angew. Chem. Int. Edn* **46**, 3269–3274 (2007).
- Vemula, P. K., Aslam, U., Mallia, V. A. & John, G. In situ synthesis of gold nanoparticles using molecular gels and liquid crystals from vitamin-C amphiphiles. *Chem. Mater.* **19**, 138–140 (2007).
- Vemula, P. K. & John, G. Smart amphiphiles: hydro/organogelators for in situ reduction of gold. *Chem. Commun.* 2218–2220 (2006).
- Sambhy, V., MacBride, M. M., Peterson, B. R. & Sen, A. Silver bromide nanoparticle/polymer composites: Dual action tunable antimicrobial materials. *J. Am. Chem. Soc.* **128**, 9798–9808 (2006).
- Lansdown, A. B. Silver. I: Its antibacterial properties and mechanism of action. *J. Wound Care.* **11**, 125–130 (2002).
- Kenawy, E.-R., Worley, S. D. & Broughton, R. The chemistry and applications of antimicrobial polymers: A state-of-the-art review. *Biomacromolecules* **8**, 1359–1384 (2007).
- Williams, R. L., Doherty, P. J., Vince, D. G., Grashoff, G. J. & Williams, D. F. The biocompatibility of silver. *Crit. Rev. Biocompat.* **5**, 221–243 (1989).
- Berger, T. J., Spadaro, J. A., Chapin, S. E. & Becker, R. O. Electrically generated silver ions: Quantitative effects on bacterial and mammalian cells. *Antimicrob. Agents Chemother.* **9**, 357–358 (1976).
- Alt, V. *et al.* An in vitro assessment of the antibacterial properties and cytotoxicity of nanoparticulate silver bone cement. *Biomaterials* **25**, 4383 (2004).
- Podsiadlo, P. *et al.* Layer-by-layer assembly of nacre-like nanostructured composites with antimicrobial properties. *Langmuir* **21**, 11915–11921 (2005).
- Morones, J. R. *et al.* The bactericidal effect of silver nanoparticles. *Nanotechnology* **16**, 2346–2353 (2005).
- Gogoi, S. K. *et al.* Green fluorescent protein-expressing *Escherichia coli* as a model system for investigating the antimicrobial activities of silver nanoparticles. *Langmuir* **22**, 9322–9328 (2006).
- Haldar, J. An, D., de Cienfuegos, L. A., Chen, J. & Klibanov, A. M. Polymeric coatings that inactivate both influenza virus and pathogenic bacteria. *Proc. Natl Acad. Sci. USA* **103**, 17667–17671 (2006).
- Lewis, K. & Klibanov, A. M. Surpassing nature: Rational design of sterile-surface materials. *Trends Biotechnol.* **23**, 343–348 (2005).
- Naik, R. R., Stringer, S. J., Agarwal, G., Jones, S. E. & Stone, M. O. Biomimetic synthesis and patterning of silver nanoparticles. *Nature Mater.* **1**, 169–172 (2002).
- Raveendran, P., Fu, J. & Wallen, S. L. Completely 'green' synthesis and stabilization of metal nanoparticles. *J. Am. Chem. Soc.* **125**, 13940–13941 (2003).
- Yin, H. & Porter, N. A. New insights regarding the autoxidation of polyunsaturated fatty acids. *Antioxid. Redox Signal.* **7**, 170–184 (2005).
- Anastas, P. T. & Williamson, T. C. *Green Chemistry: Frontiers in Benign Chemical Syntheses and Processes* (Oxford Univ. Press, Oxford, 1998).
- Tyman, J. H. P. Non-isoprenoid long chain phenols. *Chem. Soc. Rev.* **8**, 499–537 (1979).
- John, G. & Pillai, C. K. S. Self-crosslinkable monomer from cardanol: Crosslinked beads of poly(cardanyl acrylate) by suspension polymerization. *Makromol. Chem. Rapid Commun.* **13**, 255–259 (1992).
- John, G. & Pillai, C. K. S. Synthesis and characterization of a self-crosslinkable polymer from cardanol: Autoxidation of poly(cardanyl acrylate) to crosslinked film. *J. Polym. Sci. A* **31**, 1069–1073 (1993).
- Jin, R. *et al.* Photoinduced conversion of silver nanospheres to nanoprisms. *Science* **294**, 1901–1903 (2001).
- van Gorkum, R. & Bouwman, E. The oxidative drying of alkyd paint catalysed by metal complexes. *Coordination Chem. Rev.* **249**, 1709–1728 (2005).
- Tang, L., Zhang, Y., Qian, Z. & Shen, X. The mechanism of Fe^{2+} -initiated lipid peroxidation in liposomes: The dual function of ferrous ions, the roles of the pre-existing lipid peroxides and the lipid peroxyl radical. *Biochem. J.* **352**, 27–36 (2000).
- Ahmed-Choudhury, J., Orsler, D. J. & Coleman, R. Hepatobiliary effects of tertiary-butylhydroperoxide (tBOOH) in isolated rat hepatocyte couplets. *Toxicol. Appl. Pharmacol.* **152**, 270–275 (1998).
- Yin, H., Morrow, J. D. & Porter, N. A. Identification of a novel class of endoperoxides from arachidonate autoxidation. *J. Biol. Chem.* **279**, 3766–3776 (2004).
- Esterbauer, H., Schauer, R. J. & Zollner, H. Chemistry and biochemistry of 4-hydroxynonenal, malonaldehyde and related aldehydes. *Free Radic. Biol. Med.* **11**, 81–128 (1991).
- Nath, S., Ghosh, S. K., Panigrahi, S. & Pal, T. Aldehyde assisted wet chemical route to synthesize gold nanoparticles. *Ind. J. Chem. A* **43**, 1147–1151 (2004).
- Zhang, Z., Berg, A., Levanon, H., Fessenden, R. W. & Meisel, D. On the interactions of free radicals with gold nanoparticles. *J. Am. Chem. Soc.* **125**, 7959–7963 (2003).
- Russel, A. D., Path, F. R. C. & Hugo, W. B. Antimicrobial activity and action of silver. *Prog. Med. Chem.* **31**, 351–370 (1994).
- Zachariadis, P. C. *et al.* Synthesis, characterization and in vitro study of the cytostatic and antiviral activity of new polymeric silver(I) complexes with ribbon structures derived from the conjugated heterocyclic thioamide 2-mercapto-3,4,5,6-tetrahydroimidine. *Eur. J. Inorg. Chem.* **2004**, 1420–1426 (2004).
- Sondi, I. & Salopek-Sondi, B. Silver nanoparticles as antimicrobial agent: a case study on *E. coli* as a model for Gram-negative bacteria. *J. Colloid Interface Sci.* **275**, 177–182 (2004).
- Sudhir, K. Preparation, characterization, and surface modification of silver particles. *Langmuir* **14**, 1021–1025 (1998).

Acknowledgements

J. Haldar from MIT is acknowledged for discussions. A. Janakiraman, Department of Biology, CCNY is acknowledged for assisting with the microbial experiments. G.J. acknowledges the Science Interdepartmental Electron Microscope and Imaging Center at CCNY. P.M.A. acknowledges funding from NSEC at RPI. Correspondence and requests for materials should be addressed to G.J. Supplementary Information accompanies this paper on www.nature.com/naturematerials.

Reprints and permission information is available online at <http://npg.nature.com/reprintsandpermissions/>